

A. AIMI and M. DILIGENTI (\*)

**Error analysis for singular integral evaluation  
on piecewise smooth curves in Galerkin BEM (\*\*)**

*Dedicated to the memory of G. L. Braglia*

**1 - Introduction**

The formulation of certain classes of boundary value problems (potential, elasticity, fracture mechanics etc.) in terms of hypersingular boundary integral equations (HBIE) is currently gaining increasing interest; see for example ([5], [9], [12], [15], [16]). Quite often these equations are coupled with Cauchy singular boundary integral equations (CBIE).

The numerical method most frequently used to solve such type of equations is certainly the collocation method; but there are applications where the use of a Galerkin method may give some important advantages (see [11], [14], [24]). The Galerkin method however requires the user to compute efficiently integrals of the form

$$(1.1) \quad \int_{\Gamma} \bar{\phi}_j(y) \int_{\Gamma} \bar{K}(x, y) \bar{\phi}_i(x) d\Gamma_x d\Gamma_y,$$

where  $\Gamma$  is the boundary of the domain,  $\bar{\phi}_j$ ,  $\bar{\phi}_i$  are respectively test and shape functions and the kernel  $\bar{K}(x, y)$  may be of the type  $\ln r$ ,  $r^{-1}$ ,  $r^{-2}$ , with  $r = |x - y|$ .

---

(\*) Dip. di Matematica, Università di Parma, Via D'Azeglio 85, 43100 Parma, Italy.

(\*\*) Received December 2, 1998. AMS classification 65 N 38, 65 D 32.

To compute such integrals few strategies have been proposed (see [8], [9], [13]). In general they require some analytical computations or manipulations; moreover, they are either efficient but limited to particular cases of kernels, boundaries and approximants, or of wider applicability but not very efficient. To overcome these drawbacks, in [2] we have considered CBIE and HBIE defined on  $2D$  polygonal domains and proposed very efficient numerical schemes to compute the corresponding Galerkin integrals. These formulas only require the user to define a mesh on the polygonal boundary, not necessarily uniform, and specify the local degrees of the approximant; they are quite suitable for the construction of  $p$  and  $h-p$  versions of the BEM.

In [1] we have considered the case of a boundary with piecewise smooth parametric representation and we have shown how the quadrature formulas proposed in [2] can be used also in this more general situation, approximating the real boundary with very short linear interpolants when double integrals are defined on two consecutive elements with different parametrizations.

In this note we give error estimates for this approximation procedure in the case of weakly singular and Cauchy singular integrals, and analyse numerical examples dealing with critical situations.

## 2 - Evaluation of the Galerkin matrix elements

We assume that the boundary  $\Gamma$  in (1.1) is a piecewise smooth closed curve in  $\mathfrak{R}^2$ ; further, we assume that  $\Gamma$  can be decomposed as  $\Gamma = \bigcup_{l=1}^M \Gamma_l$ , where each piece  $\Gamma_l$  is the image of a one-to-one smooth map  $f_l$  defined on a closed interval  $I_l \subset \mathfrak{R}$ . In particular we define  $x \equiv (\xi_1, \xi_2) \in \Gamma_l$  by

$$\xi_1 = f_{l,1}(t), \quad \xi_2 = f_{l,2}(t), \quad t \in I_l.$$

A partition of  $I_l$  ( $I_l^k, k = 1, \dots, n_l$ ) will define a corresponding partition of  $\Gamma_l$  ( $\Gamma_l^k, k = 1, \dots, n_l$ ).

Let us also assume that on the boundary  $\Gamma$  of our problem we have defined a mesh or partition, not necessarily uniform, obtained as image of a partition of  $I = \bigcup_{l=1}^M I_l$ . Let  $e_m$  be an element of the mesh on  $\Gamma$ , image of the element  $(a_m, b_m)$  of the partition of  $I$ . By  $\{\phi_i\}$  we denote a (global) Lagrange basis relative to the partition of  $I$ . The local Lagrange basis, of degree  $d_m$ , defined on the element  $(a_m, b_m)$  will be denoted by  $\{\phi_i^{(m)}\}$ . The corresponding bases on  $\Gamma$  will be  $\{\bar{\phi}_i\}$

and  $\{\bar{\phi}_i^{(m)}\}$  where:

$$\begin{aligned}\bar{\phi}_i(x) &= \phi_i \circ f_i^{-1}(x) & \text{if } x \in \Gamma_l \\ \bar{\phi}_i^{(m)}(x) &= \phi_i^{(m)} \circ f_i^{-1}(x) & \text{if } x \in \Gamma_l.\end{aligned}$$

The elements of the Galerkin matrix contain double integrals of the form

$$(2.1) \quad \int_{\Gamma} \bar{\phi}_j(y) \int_{\Gamma} \bar{K}(y, x) \bar{\phi}_i(x) d\Gamma_x d\Gamma_y,$$

where the kernel  $\bar{K}$  can be weakly singular, singular or hypersingular. In the latter two cases the inner integral in (2.1) ought to be defined as a Cauchy principal value and as Hadamard finite part, respectively.

Further, integral (2.1) can be decomposed as the sum of double integrals of the form

$$(2.2) \quad \int_{e_m} \bar{\phi}_j^{(m)}(y) \int_{\Gamma} \bar{K}(y, x) \bar{\phi}_i(x) d\Gamma_x d\Gamma_y,$$

Since  $e_m \in \Gamma_l$  for some  $l$ , by introducing the corresponding mapping  $f_l$  the integral (2.2) can be rewritten as

$$\int_{a_m}^{b_m} \phi_j^{(m)}(s) J_{l,m}(s) \int_{\Gamma} \bar{K}(f_l(s), x) \bar{\phi}_i(x) d\Gamma_x ds,$$

where

$$J_{l,m}(s) \equiv J_m(f_l(s)) = \{[f'_{l,1}(s)]^2 + [f'_{l,2}(s)]^2\}^{1/2}, \quad a_m \leq s \leq b_m.$$

We decompose also the inner integral in (2.2), hence reduce the evaluation of (2.1) to the computation of integrals of the form

$$(2.3) \quad \int_{a_m}^{b_m} \phi_j^{(m)}(s) J_{l,m}(s) \int_{e_n} \bar{K}(f_l(s), x) \bar{\phi}_i^{(n)}(x) d\Gamma_x ds,$$

with  $e_n \in \Gamma_k$  for some  $k$ . When the kernel is hypersingular and  $e_n \equiv e_m$ , this decomposition is possible, however, only if we define both the inner and the outer integrals in (2.3) as finite parts, while if  $e_m$  and  $e_n$  are consecutive, only the outer integral in (2.3) must be defined in the finite part sense. Indeed, in such cases, the outer integral, which exists as an ordinary (improper) integral when the inner one is considered on the whole boundary  $\Gamma$ , is not defined on a single boundary ele-

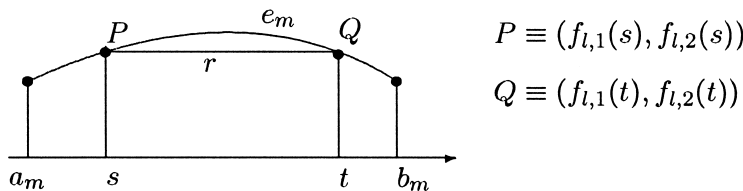
ment unless the product  $\overline{\phi}_j^{(m)}\overline{\phi}_i^{(n)}$  vanishes at those endpoints where the kernel  $\overline{K}$  becomes hypersingular. For instance this is the case when  $e_m = e_n$ ,  $i = j$  and  $\overline{\phi}_i^{(n)}(x)$  does not vanish at both endpoints of the element  $e_n$ . Notice that in the above situations the outer integral diverges if considered as an ordinary integral, since the inner one gives rise to a not integrable singularity at one or both endpoints of the outer element of integration, while the sum over all elements of  $\Gamma$  has a finite value. This remark, which has been made for the first time in [6], is vital if we want to overcome the numerical cancellation phenomenon that otherwise would naturally arise when we evaluate (2.3) by a quadrature rule and sum the contributions of all boundary elements. In other words, by defining the outer integral as stated above, we eliminate a priori (and analitically) the singular terms that would otherwise arise and that ought anyway cancel out each other in the final answer. Numerical experiments have shown that in such cases numerical cancellation can be quite dramatic, particularly when we require high accuracy. Finally, since in (2.3) the point  $y = f_i(s)$  is either outside the element  $e_n$  or in its interior (this happens only when  $e_n \equiv e_m$ ), the introduction of the change of variable  $x = f_k(t)$  is allowed and we obtain the new representation

$$(2.4) \quad \int_{a_m}^{b_m} \phi_j^{(m)}(s) J_{l,m}(s) \int_{a_n}^{b_n} K(s, t) \phi_i^{(n)}(t) J_{k,n}(t) dt ds,$$

where we have set  $K(s, t) \equiv \overline{K}(f_i(s), f_k(t))$ .

Since the kernel  $\overline{K}(y, x)$  is of the type (I)  $\ln r$ , (II)  $r^{-1}$ , (III)  $r^{-2}$ , integrals which cause difficulties, i.e., those which cannot be evaluated efficiently by the product of two Gauss-Legendre formulas, are those associated with elements  $e_m, e_n$  which are either coincident or consecutive. In these critical cases the distance  $r$  can be expressed respectively in the following forms:

Case (i):  $e_m \equiv e_n \in \Gamma_l$



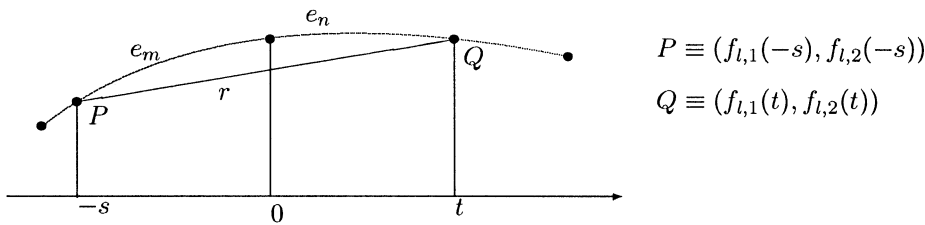
$$(2.5) \quad r^2 = [f_{l,1}(t) - f_{l,1}(s)]^2 + [f_{l,2}(t) - f_{l,2}(s)]^2 = (t - s)^2 F_1(t, s),$$

where

$$F_1(t, s) = \begin{cases} \left[ \frac{f_{l,1}(t) - f_{l,1}(s)}{t - s} \right]^2 + \left[ \frac{f_{l,2}(t) - f_{l,2}(s)}{t - s} \right]^2, & t \neq s, \\ (J_{l,m}(s))^2, & t = s \end{cases}$$

has one degree of smoothness less than that of  $f_{l,1}$  and  $f_{l,2}$ , and is always positive.

Case (ii<sub>a</sub>):  $e_m, e_n$  consecutive with the same parametrization  $f_l$ :



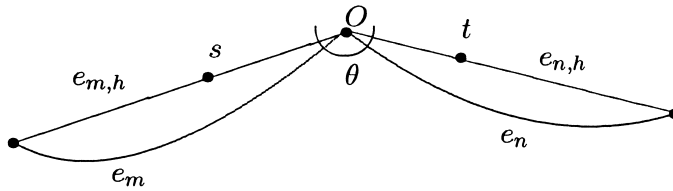
$$(2.6) \quad r^2 = [f_{l,1}(t) - f_{l,1}(-s)]^2 + [f_{l,2}(t) - f_{l,2}(-s)]^2 = (t + s)^2 F_2(t, s),$$

where

$$F_2(t, s) = \begin{cases} \left[ \frac{f_{l,1}(t) - f_{l,1}(-s)}{t + s} \right]^2 + \left[ \frac{f_{l,2}(t) - f_{l,2}(-s)}{t + s} \right]^2, & t \neq -s, \\ (J_{l,m}(-s))^2, & t = -s = 0 \end{cases}$$

has one degree of smoothness less than that of  $f_{l,1}$  and  $f_{l,2}$ , and is always positive.

Case (ii<sub>b</sub>):  $e_m, e_n$  consecutive but with a different parametrization:



We replace  $e_m, e_n$  by their linear interpolants  $e_{m,h}, e_{n,h}$ ; therefore we have the

following expression of the distance:

$$(2.7) \quad r^2 = (t - a_s)^2 + b_s^2$$

with  $a_s = s(l_m/l_n) \cos(\theta)$  and  $b_s = s(l_m/l_n) \sin(\theta)$ , having denoted with  $l_m = b_m - a_m$  the length of the interval  $(a_m, b_m)$  associated with the element  $e_m$  (see (2.4)).

Analogously, we can replace each (curved) element by a quadratic interpolant instead of a linear one, proceeding as follows. Having chosen three points  $(x_i, y_i)$ ,  $i = 1, 2, 3$  on  $e_n$ , we can define a parametric representation of the parabola:

$$\begin{aligned} x(t) &= \underline{N}^t(t) \underline{x}, \\ y(t) &= \underline{N}^t(t) \underline{y}, \quad -1 \leq t \leq 1, \end{aligned}$$

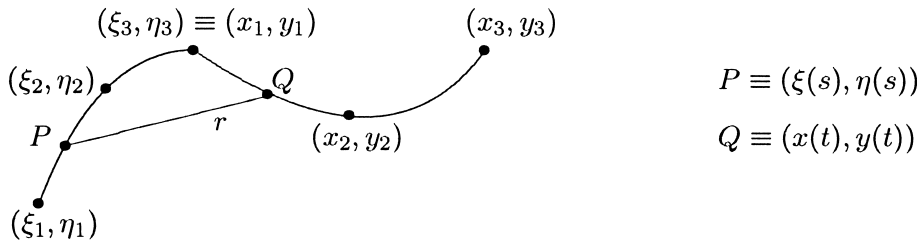
where

$$\underline{x} = (x_1, x_2, x_3)^t, \quad \underline{y} = (y_1, y_2, y_3)^t,$$

$$\underline{N}(t) = (N_1(t), N_2(t), N_3(t))^t,$$

$$N_1(t) = \frac{1}{2}t(t - 1), \quad N_2(t) = (1 - t)(t + 1), \quad N_3(t) = \frac{1}{2}t(t + 1).$$

Doing the same for the element  $e_m$ , then we define



with

$$\xi(s) = N_1(s) \xi_1 + N_2(s) \xi_2 + N_3(s) \xi_3,$$

$$\eta(s) = N_1(s) \eta_1 + N_2(s) \eta_2 + N_3(s) \eta_3$$

and

$$x(t) = N_1(t) x_1 + N_2(t) x_2 + N_3(t) x_3,$$

$$y(t) = N_1(t) y_1 + N_2(t) y_2 + N_3(t) y_3.$$

A simple calculation gives:

$$r^2 = r_1^2 + r_2^2,$$

where

$$r_1 = a_0 t^2 + a_1 s^2 + a_2 t + a_3 s + a_4,$$

$$r_2 = b_0 t^2 + b_1 s^2 + b_2 t + b_3 s + b_4,$$

with

$$\begin{cases} a_0 = \frac{1}{2}(x_1 - 2x_2 + x_3), & b_0 = \frac{1}{2}(y_1 - 2y_2 + y_3), \\ a_1 = -\frac{1}{2}(\xi_1 - 2\xi_2 + \xi_3), & b_1 = -\frac{1}{2}(\eta_1 - 2\eta_2 + \eta_3), \\ a_2 = \frac{1}{2}(x_3 - x_1), & b_2 = \frac{1}{2}(y_3 - y_1), \\ a_3 = \frac{1}{2}(\xi_1 - \xi_3), & b_3 = \frac{1}{2}(\eta_1 - \eta_3), \\ a_4 = x_2 - \xi_2, & b_4 = y_2 - \eta_2. \end{cases}$$

Therefore we have:

$$r^2 = A_0 t^4 + A_1 t^3 + A_2 t^2 + A_3 t + A_4,$$

where the  $A_i$  are known functions of  $s$ :

$$A_0 = a_0^2 + b_0^2,$$

$$A_1 = 2a_0 a_2 + 2b_0 b_2,$$

$$A_2 = s^2(2a_0 a_1 + 2b_0 b_1) + s(2a_0 a_3 + 2b_0 b_3) + (a_2^2 + 2a_0 a_4 + 2b_0 b_4 + b_2^2),$$

$$A_3 = s^2(2a_1 a_2 + 2b_1 b_2) + s(2a_2 a_3 + 2b_2 b_3) + (2a_2 a_4 + 2b_2 b_4),$$

$$A_4 = s^4(a_1^2 + b_1^2) + s^3(2a_1 a_3 + 2b_1 b_3) + s^2(a_3^2 + 2a_1 a_4 + 2b_1 b_4 + b_3^2)$$

$$+ s(2a_3 a_4 + 2b_3 b_4) + (a_4^2 + b_4^2)$$

that is, having set  $B_i = A_i/A_0$ ,  $i = 1, \dots, 4$ ,

$$(2.8) \quad r^2 = A_0(t^4 + B_1 t^3 + B_2 t^2 + B_3 t + B_4).$$

Equation (2.8) can be transformed, by the substitution  $t = y - B_1/4$ , into:

$$r^2 = A_0(y^4 + py^2 + qy + d)$$

with:  $p = -\frac{3}{8}B_1^2 + B_2$ ,  $q = \frac{1}{8}B_1^3 - B_1B_2/2 + B_3$ ,  $d = -\frac{3}{256}B_1^4 + B_1^2B_2/2 - B_1B_3/4 + B_4$ .

A cumbersome, but straightforward manipulation, leads to the factorization:

$$(2.9) \quad r^2 = A_0[(t - \alpha_1)^2 + \beta_1^2][(t - \alpha_2)^2 + \beta_2^2]$$

which contains factors of the same type of (2.7), where

$$\alpha_1 = \frac{B_1}{4} + \frac{z}{2}, \quad \beta_1^2 = \frac{4(u - zv) - z^2}{4},$$

$$\alpha_2 = \frac{B_1}{4} - \frac{z}{2}, \quad \beta_2^2 = \frac{4v - z^2}{4},$$

$$v = \frac{1}{2z}(z^3 + pz + q),$$

$$u = p + z^2 + \frac{1}{2}(z^3 + pz + q)\left(1 - \frac{1}{z}\right),$$

$$z = \frac{uv - d}{v^2}$$

and  $z$  is solution of the following equation:  $z^6 + 2pz^4 + (p^2 - 4d)z^2 - q^2 = 0$ .

We recall that in the situation described in case (ii<sub>b</sub>), if the solution of the integral equation has a «singularity» at the point 0, an  $h - p$  strategy will take elements  $e_m, e_n$  with length much shorter than those of the elements where the solution is smooth. Otherwise, we will take anyway elements  $e_m, e_n$  of small lengths. Therefore the above linear or quadratic interpolations should cause a negligible error, which will be studied in the next Section. Notice that we propose to replace  $e_m, e_n$  by their interpolants only when we consider double integrals defined over these consecutive elements, not in all other cases: we introduce this interpolation simply to approximate the specific integral and not the boundary.

Using the above expressions (2.5), (2.6), (2.7) or (2.9) of  $r$  in terms of the parameters  $s, t$  and basic quadrature rules such as product rules of interpolatory type for logarithmic and rational kernels ([2]) and the DE-rule ([20]) in [1] we have shown how to evaluate integrals of type (2.4) with numerical quadrature

schemes of the form

$$\int_0^1 \int_0^1 K(s, t) f(s, t) dt ds \approx \sum_{k=-N}^N w_k^{\text{DE}} \sum_{i=1}^n w_i^I(s_k^{\text{DE}}) f(s_k^{\text{DE}}, t_i^I)$$

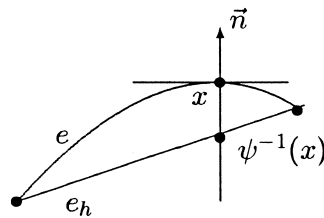
where  $\{s_k^{\text{DE}}\}$ ,  $\{w_k^{\text{DE}}\}$  are nodes and weights of the DE-rule, and  $\{t_i^I\}$ ,  $\{w_i^I(s_k^{\text{DE}})\}$  are nodes and weights of product rules. Note that these last weights depend on the outer node of integration.

### 3 - Estimates of the perturbations caused by the linearization of two consecutive elements

In Section 2 we have remarked that when we have to deal with double integrals defined on two consecutive elements with a different parametrization we replace them either by linear or by quadratic interpolants, hence proceed with these latter to compute the (approximate) Galerkin integrals.

Here we examine the behaviour of the errors generated when two consecutive elements are replaced by their linear interpolants. In particular we show that for kernels of type  $\ln r$  and  $r^{-1}$  the errors produced in the Galerkin integrals by these boundary approximants are of order  $O(h^2)$ ,  $h$  being the maximum size of the partition  $I_l^k$  ( $l = 1, \dots, M$ ;  $k = 1, \dots, n_l$ ). The case of quadratic elements is much more cumbersome and we omit it.

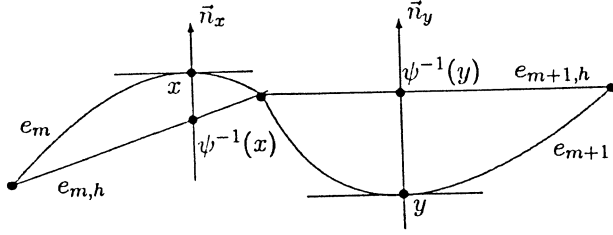
Given a curved element  $e$ , and having defined its linear interpolant  $e_h$ , we introduce the one-to-one function  $\psi$  between  $e_h$  and  $e$ . Given any  $x \in e$ ,  $\psi^{-1}(x)$  is the point of  $e_h$  which lies on the normal to  $e$  at  $x$ . At the endpoints of  $e$  we have  $\psi^{-1}(x) = x$ .



We consider the following situation:

$$e_m \in \Gamma_l, \quad e_{m+1} \in \Gamma_{l+1}$$

$$r = |x - y|, \quad \bar{r} = |\psi^{-1}(x) - \psi^{-1}(y)|$$



By replacing  $e_m, e_{m+1}$  by  $e_{m,h}, e_{m+1,h}$ , in the case of the  $\ln r$  kernel we produce the error:

$$E_1 = \left| \int_{e_{m+1}} \bar{\phi}_j^{(m+1)}(y) \int_{e_m} \ln r \bar{\phi}_i^{(m)}(x) d\Gamma_x d\Gamma_y - \int_{e_{m+1,h}} \bar{\phi}_{j,h}^{(m+1)}(y) \int_{e_{m,h}} \ln \bar{r} \bar{\phi}_{i,h}^{(m)}(x) dx dy \right|$$

where  $\{\bar{\phi}_{i,h}^{(n)}\}$  denotes the basis elements corresponding to  $\{\bar{\phi}_i^{(n)}\}$  on  $e_{n,h}$ , that is:

$$E_1 = \left| \int_{a_{m+1}}^{b_{m+1}} \phi_j^{(m+1)}(s) \int_{a_m}^{b_m} \ln \left| \psi \circ f_{m+1}^h(s) - \psi \circ f_m^h(t) \right| \phi_i^{(m)}(t) J_{m+1}(\psi \circ f_{m+1}^h(s)) J_m(\psi \circ f_m^h(t)) dt ds \right. \\ \left. + \int_{a_{m+1}}^{b_{m+1}} \phi_j^{(m+1)}(s) \int_{a_m}^{b_m} \ln |f_{m+1}^h(s) - f_m^h(t)| \phi_i^{(m)}(t) J_{m+1}(f_{m+1}^h(s)) J_m(f_m^h(t)) dt ds \right|,$$

where  $f_m^h: [a_m, b_m] \rightarrow e_{m,h}$  is a smooth map and  $\psi \circ f_m^h(s) = \psi((f_{m,1}^h(s), f_{m,2}^h(s))^t)$ . Then we rewrite  $E_1$  as follows:

$$(3.1) \quad E_1 = \left| \int_{a_{m+1}}^{b_{m+1}} \phi_j^{(m+1)}(s) \int_{a_m}^{b_m} \ln \left| \psi \circ f_{m+1}^h(s) - \psi \circ f_m^h(t) \right| \phi_i^{(m)}(t) \right. \\ \left. [J_{m+1}(\psi \circ f_{m+1}^h(s)) J_m(\psi \circ f_m^h(t)) - J_{m+1}(f_{m+1}^h(s)) J_m(f_m^h(t))] dt ds + \right. \\ \left. \int_{a_{m+1}}^{b_{m+1}} \phi_j^{(m+1)}(s) J_{m+1}(f_{m+1}^h(s)) \int_{a_m}^{b_m} \ln \frac{|\psi \circ f_{m+1}^h(s) - \psi \circ f_m^h(t)|}{|f_{m+1}^h(s) - f_m^h(t)|} \phi_i^{(m)}(t) J_m(f_m^h(t)) dt ds \right|.$$

The quantity contained in the square bracket in (3.1):

$$A = J_{m+1}(\psi \circ f_{m+1}^h(s)) J_m(\psi \circ f_m^h(t)) - J_{m+1}(f_{m+1}^h(s)) J_m(f_m^h(t))$$

can be bounded by:

$$\begin{aligned} |A| &\leq |J_m(\psi \circ f_m^h(t))| \cdot |J_{m+1}(\psi \circ f_{m+1}^h(s)) - J_{m+1}(f_{m+1}^h(s))| \\ &\quad + |J_{m+1}(f_{m+1}^h(s))| \cdot |J_m(\psi \circ f_m^h(t)) - J_m(f_m^h(t))|, \end{aligned}$$

hence, because of (2.12) in ([21], Lemma 3), by:

$$\begin{aligned} &|J_m(\psi \circ f_m^h(t))| C_1 h^2 \sup_{a_{m+1} \leq s \leq b_{m+1}} |D^2 f_{l+1}(s)| \\ &+ |J_{m+1}(f_{m+1}^h(s))| C_2 h^2 \sup_{a_m \leq t \leq b_m} |D^2 f_l(t)|. \end{aligned}$$

By assuming the parametrization functions  $f_j$  of class  $C^2(\bar{\Gamma}_j)$ , we finally obtain:

$$|A| \leq Ch^2.$$

The quantity:

$$\ln \left| \frac{\psi \circ f_{m+1}^h(s) - \psi \circ f_m^h(t)}{f_{m+1}^h(s) - f_m^h(t)} \right|$$

is uniformly bounded for all values of  $a_{m+1} \leq s \leq b_{m+1}$ ,  $a_m \leq t \leq b_m$  (see [21], (2.13)).

Therefore we have:

$$\begin{aligned} (3.2) \quad E_1 &\leq C_1 h^2 \int_{a_{m+1}}^{b_{m+1}} |\phi_j^{(m+1)}(s)| \int_{a_m}^{b_m} |\ln |\psi \circ f_{m+1}^h(s) - \psi \circ f_m^h(t)|| \cdot |\phi_i^{(m)}(t)| dt ds \\ &+ C_2 \int_{a_{m+1}}^{b_{m+1}} |\phi_j^{(m+1)}(s)| |J_{m+1}(f_{m+1}^h(s))| \int_{a_m}^{b_m} |\phi_i^{(m)}(t)| |J_m(f_m^h(t))| dt ds. \end{aligned}$$

Since the first term in (3.2) defines a continuous bilinear form on  $L^2(\Gamma_l) \times L^2(\Gamma_{l+1})$ , and each  $|J(\cdot)|$  is uniformly bounded by a constant, from (3.2) we have:

$$E_1 \leq \bar{C}_1 h^2 \|\bar{\phi}_j^{(m+1)}\|_{L^2(\Gamma_{l+1})} \cdot \|\bar{\phi}_i^{(m)}\|_{L^2(\Gamma_l)} + \bar{C}_2 h^2 \|\phi_j^{(m+1)}\|_{L^\infty(a_{m+1}, b_{m+1})} \cdot \|\phi_i^{(m)}\|_{L^\infty(a_m, b_m)},$$

that is:

$$(3.3) \quad E_1 \leq Ch^2.$$

In the case of the  $r^{-1}$  kernel, i.e., for example,  $K(s, t) = \frac{\mathbf{n} \cdot \mathbf{r}}{r^2}$ , where  $\mathbf{n}$  is either  $\mathbf{n}_x$  or  $\mathbf{n}_y$ , we have:

$$\begin{aligned} E_2 &= \left| \int_{e_{m+1}} \overline{\phi}_j^{(m+1)}(y) \int_{e_m} \frac{\mathbf{n} \cdot \mathbf{r}}{r^2} \overline{\phi}_i^{(m)}(x) \, d\Gamma_x \, d\Gamma_y - \int_{e_{m+1, h}} \overline{\phi}_{j, h}^{(m+1)}(y) \int_{e_{m, h}} \frac{\overline{\mathbf{n}} \cdot \overline{\mathbf{r}}}{\overline{r}^2} \overline{\phi}_{i, h}^{(m)}(x) \, dx \, dy \right| \\ &= \left| \int_{a_{m+1}}^{b_{m+1}} \phi_j^{(m+1)}(s) \int_{a_m}^{b_m} \left[ \frac{\mathbf{n} \cdot \mathbf{r}}{r^2} \right]_{s, t} \phi_i^{(m)}(t) J_{m+1}(\psi \circ f_{m+1}^h(s)) J_m(\psi \circ f_m^h(t)) \, dt \, ds \right. \\ &\quad \left. - \int_{a_{m+1}}^{b_{m+1}} \phi_j^{(m+1)}(s) \int_{a_m}^{b_m} \left[ \frac{\overline{\mathbf{n}} \cdot \overline{\mathbf{r}}}{\overline{r}^2} \right]_{s, t} \phi_i^{(m)}(t) J_{m+1}(f_{m+1}^h(s)) J_m(f_m^h(t)) \, dt \, ds \right|, \end{aligned}$$

where  $[a]_{s, t}$  denotes the parametrization of  $a$ . Then we write:

$$\begin{aligned} E_2 &= \left| \int_{a_{m+1}}^{b_{m+1}} \phi_j^{(m+1)}(s) \int_{a_m}^{b_m} \left[ \frac{\mathbf{n} \cdot \mathbf{r}}{r^2} \right]_{s, t} \phi_i^{(m)}(t) \right. \\ &\quad \cdot [J_{m+1}(\psi \circ f_{m+1}^h(s)) J_m(\psi \circ f_m^h(t)) - J_{m+1}(f_{m+1}^h(s)) J_m(f_m^h(t))] \, dt \, ds \\ &\quad \left. + \int_{a_{m+1}}^{b_{m+1}} \phi_j^{(m+1)}(s) \int_{a_m}^{b_m} \left\{ \left[ \frac{\mathbf{n} \cdot \mathbf{r}}{r^2} \right]_{s, t} - \left[ \frac{\overline{\mathbf{n}} \cdot \overline{\mathbf{r}}}{\overline{r}^2} \right]_{s, t} \right\} \phi_i^{(m)}(t) J_{m+1}(f_{m+1}^h(s)) J_m(f_m^h(t)) \, dt \, ds \right|, \end{aligned}$$

and derive, using the same arguments of the  $\ln r$  case, the bound:

$$\begin{aligned} E_2 &\leq C_1 h^2 \left[ \int_{a_{m+1}}^{b_{m+1}} |\phi_j^{(m+1)}(s)| \int_{a_m}^{b_m} \left| \left[ \frac{\mathbf{n} \cdot \mathbf{r}}{r^2} \right]_{s, t} \right| \cdot |\phi_i^{(m)}(t)| \, dt \, ds \right] \\ &\quad + C_2 \left[ \int_{a_{m+1}}^{b_{m+1}} |\phi_j^{(m+1)}(s)| \int_{a_m}^{b_m} \left| \left[ \frac{\mathbf{n} \cdot \mathbf{r}}{r^2} \right]_{s, t} - \left[ \frac{\overline{\mathbf{n}} \cdot \overline{\mathbf{r}}}{\overline{r}^2} \right]_{s, t} \right| \cdot |\phi_i^{(m)}(t)| \, dt \, ds \right]. \end{aligned}$$

Notice that we also have ([21], Lemma 3):

$$\begin{aligned} \left| \left[ \frac{\mathbf{n} \cdot \mathbf{r}}{r^2} \right]_{s,t} - \left[ \frac{\bar{\mathbf{n}} \cdot \bar{\mathbf{r}}}{\bar{r}^2} \right]_{s,t} \right| &= \frac{|(\mathbf{n} \cdot \mathbf{r}) \bar{r}^2 - (\bar{\mathbf{n}} \cdot \bar{\mathbf{r}}) r^2|}{r^2 \bar{r}^2} \\ &\leq \frac{|\mathbf{n} \cdot \mathbf{r}| \bar{r}^2 + |\bar{\mathbf{n}} \cdot \bar{\mathbf{r}}| r^2}{r^2 \bar{r}^2} \leq \frac{c_1^* |\mathbf{n}| r^2 \bar{r}^2 + c_2^* |\bar{\mathbf{n}}| \bar{r}^2 r^2}{r^2 \bar{r}^2} \leq c. \end{aligned}$$

Therefore,

$$\begin{aligned} E_2 &\leq \bar{C}_1 h^2 \int_{a_{m+1}}^{b_{m+1}} |\phi_j^{(m+1)}(s)| \int_{a_m}^{b_m} \left| \left[ \frac{\mathbf{n} \cdot \mathbf{r}}{r^2} \right]_{s,t} \right| |\phi_i^{(m)}(t)| dt ds \\ &\quad + \bar{C}_2 \int_{a_{m+1}}^{b_{m+1}} |\phi_j^{(m+1)}(s)| \int_{a_m}^{b_m} |\phi_i^{(m)}(t)| dt ds. \end{aligned}$$

Finally, as in the  $\ln r$  case we obtain:

$$E_2 \leq C_1^* h^2 \|\bar{\phi}_j^{(m+1)}\|_{L^2(\Gamma_{l+1})} \cdot \|\bar{\phi}_i^{(m)}\|_{L^2(\Gamma)} + C_2^* h^2 \|\phi_j^{(m+1)}\|_{L^\infty(a_{m+1}, b_{m+1})} \cdot \|\phi_i^{(m)}\|_{L^\infty(a_m, b_m)},$$

i.e.,

$$(3.4) \quad E_2 = O(h^2).$$

#### 4 - Numerical results

In this section, some significant examples are reported in order to verify the accuracy of the numerical solution obtained with the integration schemes proposed in [1] and to analyse the error produced by the linearization of two consecutive elements with different parametrizations. In particular, we use different versions of Galerkin BEM, the classical  $h$ -version, which achieves the accuracy by refining the mesh while using low degrees  $p$  of elements, the  $p$ -version which keeps the mesh fixed and the accuracy is achieved by increasing the degree  $p$ , and the  $h-p$  version which combines both approaches.

Example 1. We consider the following Dirichlet problem: for given  $u_0 \in H^{1/2}$  find  $u$  satisfying:

$$(4.1) \quad \nabla^2 u = 0 \quad \text{in } \mathfrak{R}^2 - \Gamma, \quad u = u_0 \quad \text{on } \Gamma, \quad u = O\left(\frac{1}{|x|}\right) \quad \text{as } |x| \rightarrow \infty$$

where  $\Gamma$  is an open arc (smooth piece of a curve) non-intersecting itself.

For problem (4.1), an existence and uniqueness result [22] holds; moreover, it can be reduced to a weakly singular integral equation of the first kind:

$$(4.2) \quad -\frac{1}{2\pi} \int_{\Gamma} \Delta q(y) \ln|x-y| d\Gamma_y = u_0(x), \quad x \in \Gamma.$$

In this example we consider  $u_0 = \frac{1}{4\pi} \ln 2$  and  $\Gamma$  the semi-circular arc  $\{(x_1, x_2), x_1 = \cos \theta, x_2 = \sin \theta, 0 < \theta < \pi\}$  with the true solution in polar coordinates ([4]):

$$\Delta q(\theta) = \frac{\sqrt{2}}{4\pi} \left[ \left( \tan \frac{\theta}{2} \right)^{1/2} + \left( \cot \frac{\theta}{2} \right)^{1/2} \right].$$

We have analysed the numerical solution using the  $h-p$  version on different geometric decompositions of  $\Gamma$ . To this end, we have defined a geometric mesh  $\Gamma_\sigma^n$ , depending on a parameter  $\sigma$ ,  $0 < \sigma < 1$ , on  $\Gamma$  with nodes:

$$\begin{aligned} x_{1,0} &= 1, & x_{2,0} &= 0, \\ x_{1,i} &= \cos\left(\frac{\pi}{2} \sigma^{n+1-i}\right), & x_{2,i} &= \sin\left(\frac{\pi}{2} \sigma^{n+1-i}\right), \quad i = 1, \dots, n+1, \\ x_{1,2n+2-i} &= -x_{1,i}, & x_{2,2n+2-i} &= x_{2,i}, \quad i = 0, \dots, n. \end{aligned}$$

Denoting with  $\Delta q^N$  the computed approximate solution and with:

$$D(\Delta q) := -\frac{1}{2\pi} \int_{\Gamma} \Delta q(y) \ln|x-y| d\Gamma_y$$

in Table I we present the relative error in energy norm:

$$(4.3) \quad \|e\|_{D,r} := \frac{\|\Delta q - \Delta q^N\|_{D(\Gamma)}}{\|\Delta q\|_{D(\Gamma)}} = \left\{ \frac{\langle u_0, \Delta q - \Delta q^N \rangle_{L_2(\Gamma)}}{\langle D(\Delta q), \Delta q \rangle_{L_2(\Gamma)}} \right\}^{1/2}$$

for some values of  $\sigma$ ,  $n$  and  $p$ , this last parameter being the degree of shape functions we have used. Our numerical experiments confirm the error estimates for

TABLE I. – *The relative error in energy norm (4.3).*

$\sigma = 0.0625$								
$p$	$n = 2$		$n = 4$		$n = 6$		$n = 8$	
	$N$	$\ e\ _{D,r}$						
1	7	$0.72887E-1$	11	$0.70212E-1$	15	$0.70201E-1$	19	$0.70200E-1$
2	13	$0.37269E-1$	21	$0.33526E-1$	29	$0.33508E-1$	37	$0.335089E-1$
3	19	$0.16995E-1$	31	$0.13192E-1$	43	$0.13175E-1$	55	$0.13174E-1$
4	25	$0.10860E-1$	41	$0.60550E-2$	57	$0.60284E-2$	73	$0.60283E-2$
5	31	$0.69606E-2$	51	$0.23970E-2$	71	$0.24407E-2$	91	$0.24406E-2$
$\sigma = 0.125$								
1	7	$0.57839E-1$	11	$0.41157E-1$	15	$0.40840E-1$	19	$0.40835E-1$
2	13	$0.34843E-1$	21	$0.17332E-1$	29	$0.16796E-1$	37	$0.16789E-1$
3	19	$0.22099E-1$	31	$0.46290E-2$	43	$0.37585E-2$	55	$0.37432E-2$
4	25	$0.17587E-1$	41	$0.27392E-2$	57	$0.32977E-2$	73	$0.25144E-2$
5	31	$0.14429E-1$	51	$0.11765E-2$	71	$0.24993E-2$	91	$0.33056E-2$
$\sigma = 0.5$								
1	7	$0.16349E+0$	11	$0.83058E-1$	15	$0.41712E-1$	19	$0.20936E-1$
2	13	$0.11207E+0$	21	$0.56374E-1$	29	$0.28128E-1$	35	$0.13856E-1$
3	19	$0.85618E-1$	31	$0.42899E-1$	43	$0.21322E-1$	53	$0.10362E-1$
4	25	$0.69467E-1$	41	$0.34729E-1$	57	$0.17192E-1$	71	$0.82203E-2$
5	31	$0.58484E-1$	51	$0.29185E-1$	71	$0.14380E-1$	89	$0.67357E-2$

the  $h-p$  version for geometric mesh given in [22] for Dirichlet problem:

$$(4.4) \quad \|\Delta q - \Delta q^N\|_{H^{1/2}} \leq C e^{-b\sqrt{N}}$$

where  $N$  is the number of degrees of freedom,  $C$  and  $b$  are some positive constants depending on  $\sigma$  but not on  $N$ . In Figure 1, 2 and 3, we compare some of the previous results in the  $\sqrt{N} - \ln\|e\|_{D,r}$  scale; in particular, Figure 1 ( $n = 4$ ) and Figure 2 ( $n = 8$ ) show that the error decays exponentially with increasing degree  $p$  of the shape functions (and therefore, with increasing number  $N$  of degrees of freedom) when the number of grid-points is kept fixed; the speed of convergence clearly depends on  $\sigma$ . Figure 3 shows that when we keep  $p$  fixed ( $p = 5$ ), and

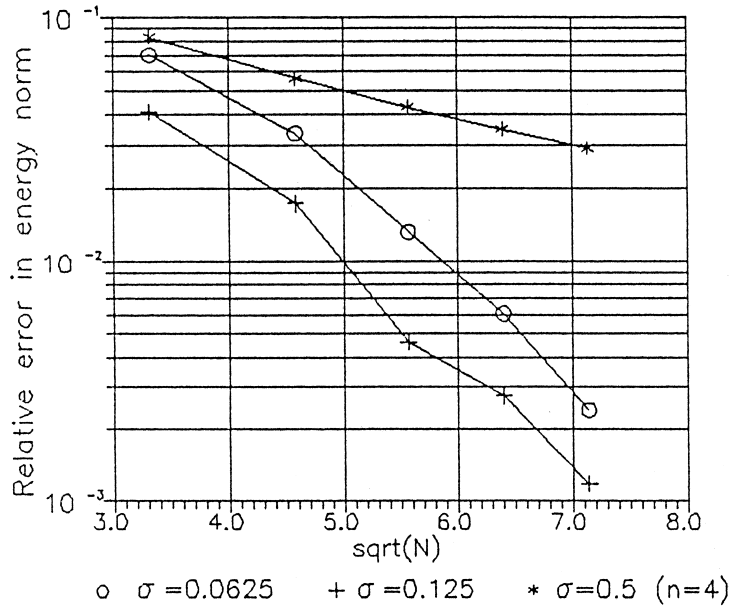


Figure 1.

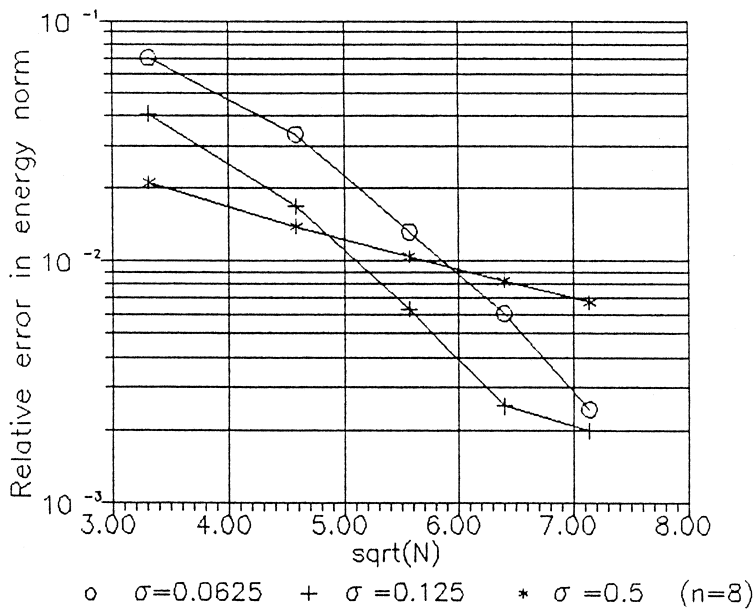


Figure 2.

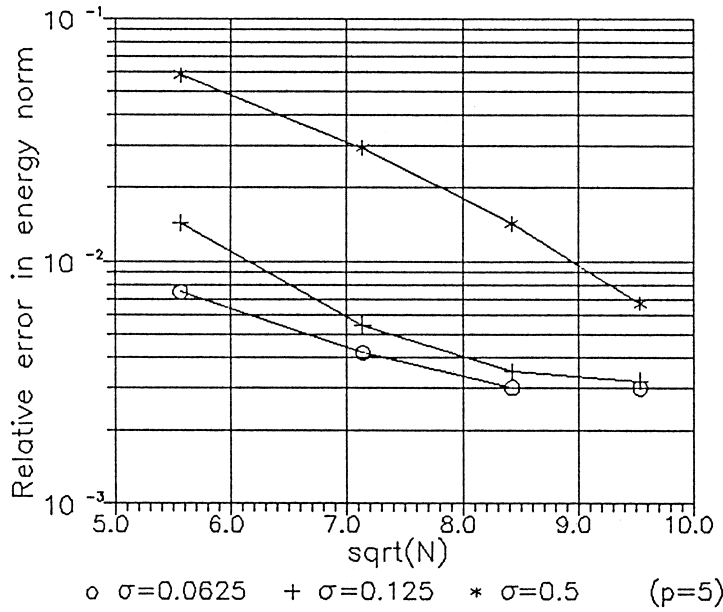


Figure 3.

choose for example  $\sigma = 0.0625$  and  $\sigma = 0.125$ , the rate of convergence is not exponential; for  $\sigma = 0.0625$  we obtain the best results.

Example 2. This problem involves the solution of the Laplace equation in a circular domain of radius  $R$  subject to the boundary conditions shown in Figure 4. Note that there is a discontinuity of the solution for the points  $(R, 0)$  and  $(R, \pi)$ . An analytical solution of the problem can be obtained ([3]) as a Fourier series of the type:

$$\frac{u(r, \theta)}{u_0} = \frac{1}{2} + 2 \sum_{n=0}^{\infty} \frac{1}{(2n+1)\pi} \left(\frac{r}{R}\right)^{(2n+1)} \sin(2n+1)\theta.$$

We have then determined a numerical solution of this problem using the  $h-p$  version of the BEM, on different geometric decompositions of  $\Gamma$  taking classical Lagrange polynomials with degree  $p$  varying from 1 to 3 as interpolation

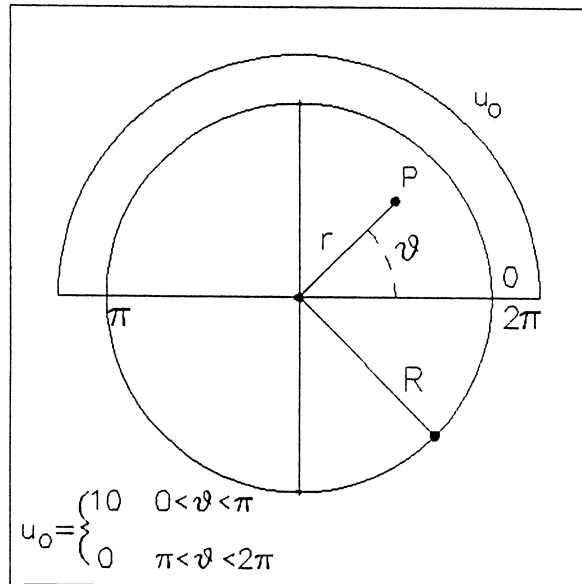


Figure 4. - The problem of Example 2 with the boundary conditions.

functions. We have defined a geometric mesh  $\Gamma_\sigma^n$  ( $0 < \sigma < 1$ ) on  $\Gamma$  with nodes generated by the following decomposition of the interval  $[0, 2\pi)$ :

$$t_0 = 0,$$

$$t_i = \frac{\pi}{2} \sigma^{n+1-i}, \quad i = 1, \dots, n+1,$$

$$t_{n+1+i} = \pi - t_{n+1-i}, \quad i = 1, \dots, n+1,$$

$$t_{2n+2+i} = \pi + \frac{\pi}{2} \sigma^{n+1-i}, \quad i = 1, \dots, n+1,$$

$$t_{3n+3+i} = 2\pi - t_{n+1-i}, \quad i = 1, \dots, n+1.$$

Results for some internal points (Figure 5) are compared in Table II for  $\sigma = 0.25$ ,  $n = 3$ , and  $p = 1, 2, 3$ , assuming  $u_0 = 10$  and  $R = 2$ . Since the analytical solution is expanded as a sine series, it is not capable of predicting the distribution of fluxes. The boundary fluxes present a singularity; the numerical results, for several discretizations tend to represent this singularity as shown in Figure 6.

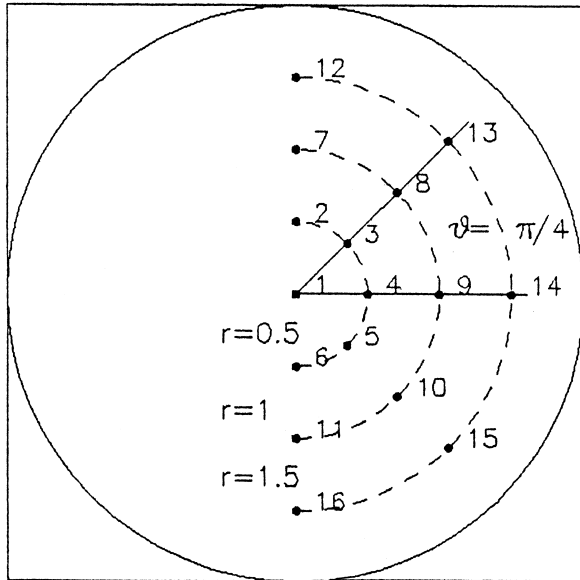


Figure 5. - Internal points.

TABLE II. - Comparison for some internal points (Figure 5).

$\sigma = 0.25 \quad n = 3$									
Point	Analytical	$p = 1$	$p = 2$	$p = 3$	Point	Analytical	$p = 1$	$p = 2$	$p = 3$
1	5.0000	5.0000	5.0000	5.0000	9	5.0000	5.0000	5.0000	5.0000
2	6.5596	6.5599	6.5596	6.5596	10	2.5937	2.5924	2.5937	2.5937
3	6.1479	6.1483	6.1479	6.1483	11	2.0483	2.0488	2.0483	2.0483
4	5.0000	5.0000	5.0000	5.0000	12	9.0967	9.0881	9.0967	9.0967
5	3.8521	3.8517	3.8520	3.8521	13	8.7547	8.7596	8.7547	8.7547
6	3.4404	3.4401	3.4404	3.4404	14	5.0000	5.0000	5.0000	5.0000
7	7.9517	7.9512	7.9517	7.9517	15	1.2453	1.2404	1.2452	1.2453
8	7.4063	7.4076	7.4063	7.4063	16	0.9033	0.9119	0.9033	0.9033

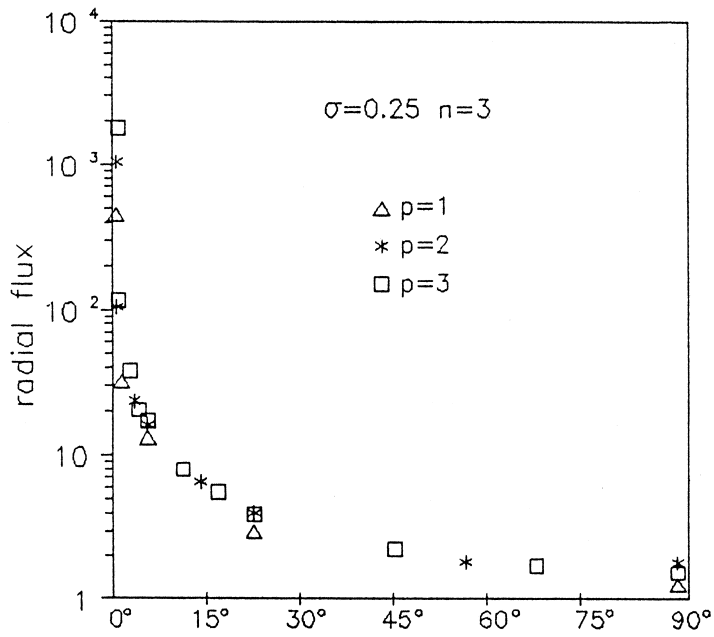


Figure 6. - Results for the radial fluxes.

Example 3. Again, in this example the boundary condition provided everywhere is potential, with the normal gradients as unknowns. Figure 7 shows the domain employed: its boundary  $\Gamma$  is formed by four circular arcs, centred

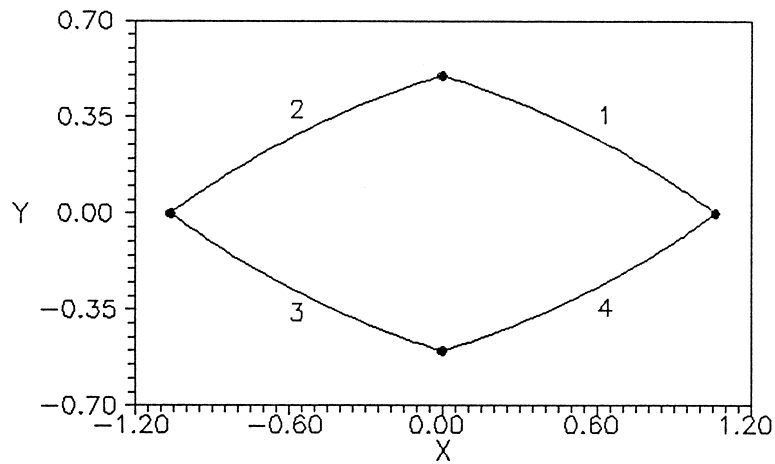


Figure 7. - Domain of Example 3.

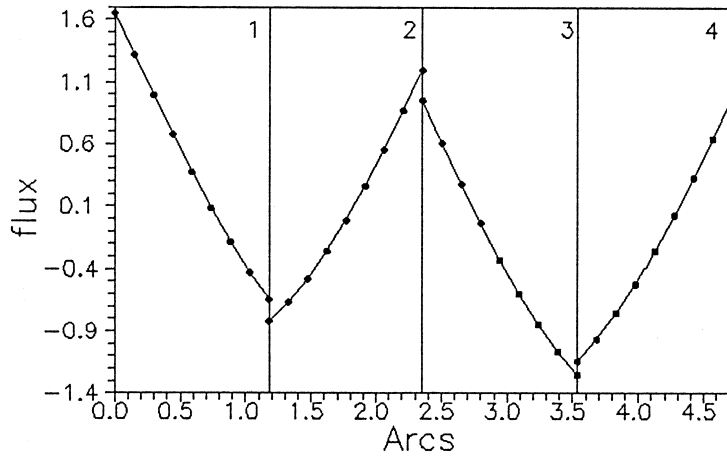


Figure 8. - Numerical approximation of flux on  $\Gamma$ .

respectively at  $(1, 3)$ ,  $(-1, 3)$ ,  $(1, -3)$  and  $(-1, -3)$ , each of radius 3.64. The potential distribution over the domain is

$$u(x, y) = \ln \{(x - 2)^2 + (y - 2)^2\}^{-0.5} + x^2 - y^2.$$

Figure 8 shows, on the four arcs of  $\Gamma$ , the analytical gradients and the numerical approximation of the flux obtained with a uniform decomposition of the boundary

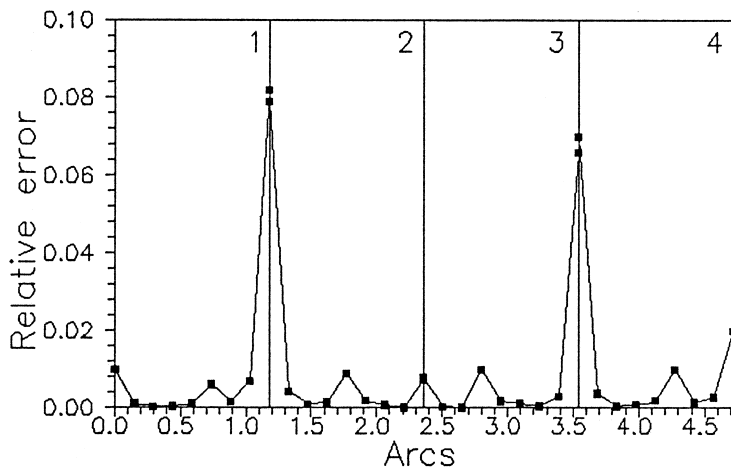


Figure 9. - Relative error of Example 3.

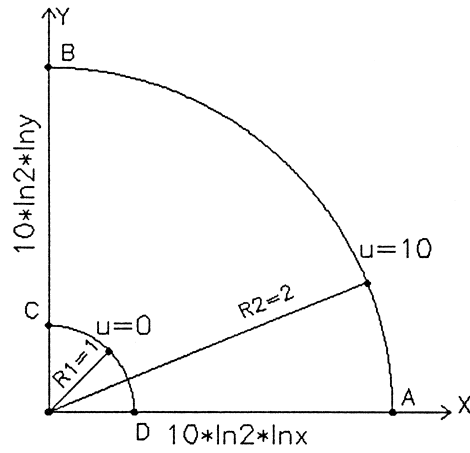


Figure 10. - Example 4: geometry and boundary conditions.

in 32 elements, using linear shape functions. In Figure 9 nodal relative errors between the exact and the numerical solutions are plotted: here we note that, as it is obvious, the maximum error occurs at the junction point between different arcs, where we have evaluated the corresponding double integrals substituting the real boundary with its linear interpolant, and specially where the datum has greater magnitude; in the middle of each arc, errors are much smaller. Further,

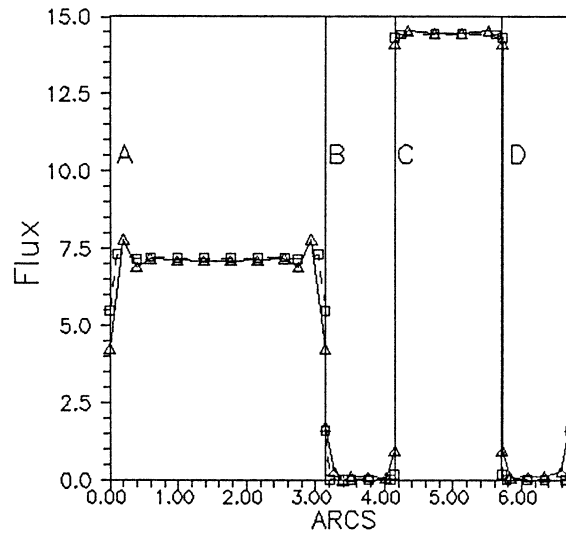


Figure 11. -  $\triangle h = 0.2$ ,  $\square h = 0.1$ .

we observe that using more elements in the decomposition of  $\Gamma$  does not improve substantially the numerical result just presented, since the diminishing integration error is «compensated» by an increasing condition number of the final linear system, which produces a global approximation error of the same order.

Example 4. In this case the domain  $\Omega$  is represented in Fig. 10, and the Dirichlet data on  $\Gamma$  are assigned in such a way that the solution (distributed radially) is

$$u(r) = u(R_1) + \frac{u_0}{\ln(R_2/R_1)} \ln(r/R_1)$$

where  $R_1$  and  $R_2$  denote the inner and outer radius, respectively, and  $u_0 = u(R_2) - u(R_1)$ . Figure 11 shows the behaviour of the approximated flux on  $\Gamma$ , obtained with a decomposition of the boundary in 40 elements and using linear shape functions. In the vertex  $A, B, C, D$ , we have replaced the consecutive elements  $e_m, e_n$  by their linear interpolants  $e_{m,h}, e_{n,h}$  of length  $h$ . We have evaluated numerical solutions using different values of this parameter  $h$ , and we have reported in Figure 11 two of them, corresponding to  $h = 0.2$  and  $h = 0.01$ . We can observe that the second solution is better than the first at the corner points, while in the remaining parts of  $\Gamma$ , where no approximation of the boundary is introduced, the two numerical fluxes are comparable.

### References

- [1] A. AIMI, A. CARINI, M. DILIGENTI and G. MONEGATO, *Numerical integration schemes for evaluation of (hyper) singular integrals in 2D BEM*, Comput. Mech., **22** (1998), 1-11.
- [2] A. AIMI, M. DILIGENTI and G. MONEGATO, *New Numerical Integration Schemes for applications of Galerkin BEM to 2D problems*, Internat. J. Numer. Methods Engrg., **40** (1997), 1977-1999.
- [3] V. S. ARPACI, *Conduction Heat Transfer*, Addison-Wesley, Reading, Mass. 1966.
- [4] L. BANSI, *An Electrostatic Problem of a Semi-Circular Strip*, ZAMM, **59** (1979), 271-272.
- [5] T. A. CRUSE, *Boundary Element Analysis in Computational Fracture Mechanics*, Kluwer Academic, Dordrecht, The Netherlands 1988.

- [6] M. DILIGENTI and G. MONEGATO, *Integral evaluation in the BEM solution of (hyper)singular integral equations. 2D problems on polygonal domains*, J. Comput. Appl. Math., **81** (1997), 29-57.
- [7] M. DILIGENTI and G. MONEGATO, *Finite-part integrals: their occurrence and computation*, Rend. Circ. Mat. Palermo (2), **33** (1993), 39-61.
- [8] M. GUIGGIANI and P. CASALINI, *Direct computation of Cauchy Principal Value integrals in advanced Boundary Elements*, Internat. J. Numer. Methods Engrg., **24** (1987), 1711-1720.
- [9] M. GUIGGIANI, *Direct evaluation of hypersingular integrals in 2D BEM*, in Notes in Numerical Fluid Mechanics, W. Hackbusch ed., Vieweg, Vol. **33** (1992), 23-34.
- [10] J. HADAMARD, *Lectures on Cauchy's Problem in Linear Partial Differential Equations*, Yale Univ. Press, New Haven, Conn., 1923.
- [11] F. HARTMANN, C. KATZ and B. PROTOPSALTIS, *Boundary Elements and Symmetry*, Ing. Archiv., **55** (1985), 440-449.
- [12] S. HOLZER, *On the Engineering Analysis of 2D Problems by the Symmetric Galerkin Boundary Element Method and Coupled BEM/FEM*, in Advances in Boundary Element Techniques, J. H. Kane, G. Maier, N. Tosaka, S. N. Atluri (Eds.), Springer-Verlag 1993.
- [13] S. M. HOLZER, *A p-extension of the symmetric boundary element method*, Comput. Methods Appl. Mech. Engrg., **115** (1994), 339-357.
- [14] G. MAIER, G. NOVATI and S. SIRTORI, *On symmetrization in boundary element elastic and elastic-plastic analysis*, in G. Kuhn and H. Mang (Eds.), Discretization Methods in Structural Mechanics, Springer-Verlag, Berlin, 1990, 191-200.
- [15] G. MAIER, G. NOVATI and S. SIRTORI, *Symmetric formulation of indirect boundary element method for elastic-plastic analysis and relevant extremum properties*, in M. Tanaka and T. A. Cruse (Eds.), Boundary Element Methods in Applied Mechanics, Pergamon Press, Oxford, 1989, 215-224.
- [16] G. MAIER, G. NOVATI and Z. CEN, *Symmetric Galerkin boundary element method for quasi-brittle-fracture and frictional contact problems*, Comput. Mech. **13** (1993), 74-89.
- [17] G. MONEGATO, *The numerical evaluation of one-dimensional Cauchy principal value integrals*, Computing, **29** (1982), 337-354.
- [18] G. MONEGATO, *The numerical evaluation of hypersingular integrals*, J. Comput. Appl. Math., **50** (1994), 9-31.
- [19] G. MONEGATO, *The Numerical Evaluation of 2-D Cauchy Principal Value Integral Arising in Boundary Integral Equation Methods*, Math. Comp., **62**, 206 (1994), 765-777.
- [20] M. MORI, *Quadrature formulas obtained by variable transformation and the DE-rule*, J. Comput. Appl. Math., **12-13** (1985), 119-130.
- [21] J. C. NEDELEC, *Curved finite element methods for the solution of singular integral equations on surfaces in  $\mathbb{R}^3$* , Comput. Methods Appl. Mech. Engrg., **8** (1976), 61-80.
- [22] F. V. POSTEL and E. P. STEPHAN, *On the h-, p- and h-p version of the boundary element method-numerical results*, Comput. Methods Appl. Mech. Engrg., **83** (1990), 69-89.

- [23] C. SCHWAB and W. L. WENDLAND, *Kernel properties and representations of boundary integral operators*, Math. Nachr., **156** (1992), 156-218.
- [24] S. SIRTORI, G. MAIER, G. NOVATI and S. MICOLI, *A Galerkin symmetric boundary element method in elasticity: formulation and implementation*, Internat. J. Numer. Methods Engrg., **35** (1992), 255-282.

#### Abstract

*In this paper we consider integral equations associated with 2D boundary value problems defined on domains whose boundary is given by piecewise smooth parametric representations. Given any (polynomial) local basis, in a previous work ([1]) we have shown how to compute efficiently all integrals required by the Galerkin method, substituting the real boundary with short linear interpolants when double integrals are defined on two consecutive elements with different parametrizations. Here we give estimates for the error generated by this approximation procedure in weakly singular and Cauchy singular integrals and analyse numerical examples, not previously shown, dealing with critical cases.*

\*\*\*